Available online at www.sciencedirect.com
SCIENCE DIRECT®

Journal of Hydrology 314 (2005) 275–288

Journal of Hydrology

www.elsevier.com/locate/jhydrol

Recent advances in wavelet analyses: Part 1. A review of concepts

David Labat*

Laboratoire des Mécanismes et Transferts en Géologie (LMTG), UMR 5563, CNRS/IRD/UPS, 14 Ave. E. Belin, Toulouse 31400, France

Received 28 May 2003; revised 15 March 2005; accepted 1 April 2005

Abstract

This contribution provides a review of the most recent wavelet applications in the field of earth sciences and is devoted to introducing and illustrating new wavelet analysis methods in the field of hydrology. Wavelet analysis remains unknown in the field of hydrology even though it clearly overcomes the well-known limits of the classical Fourier analysis. New wavelet-based tools are proposed to hydrologists in order to make wavelet analysis more attractive. First, a multiresolution continuous wavelet analysis method is shown to significantly improve the determination of the temporal-scale structure of a given signal. Second, the concept of wavelet entropy in both continuous and multiresolution frameworks is introduced allowing for an estimation of the temporal evolution of a given hydrological or climatologic signal's complexity. New insights in the scale-dependence of the relationship are exposed by introducing wavelet cross-correlation and wavelet coherence. Continuous wavelet cross-correlation provides a time–scale distribution of the correlation between two signals, whereas continuous wavelet coherence provides a qualitative estimator of the temporal evolution of the degree of linearity of the relationship between two signals on a given scale. These methods are applied to four large river runoffs and two global climatic indexes in a companion paper.

Keywords: Wavelet analyses; Wavelet coherence; Wavelet entropy; Time–scale relationship

The widely used Fourier transform is designed for stationary signals consisting of a linear superposition of linear, independent, and non-evolving periodicities. The infinite repetition of sine and cosine functions, which constitutes the Fourier classical basis, is well suited for treatment of data involving stationary periodic processes. It is very popular in electronics, for example. However, this treatment is not well suited for data, which involves transient processes. Focusing on hydrology, signal fluctuations are highly unstationary and physical processes often operate under a large range of scales varying from one day to several decades both for rainfall rates (Mandelbrot and Wallis, 1968; Tessier et al., 1996; de Lima et al., 1999) and river discharges (Pandey, 1998; Labat et al., 2000,2002).

* Tel.: +33 5 6155 8685; fax: +33 5 6155 8138.
E-mail addresses: labat@lmtg.ups-tlse.fr (D. Labat), labat@lmtg.obs-mip.fr (D. Labat).

0022-1694/$ - see front matter © 2005 Elsevier B.V. All rights reserved.
doi:10.1016/j.jhydrol.2005.04.003

Fourier analyses have severe limitations for analysing signals that include significant departures from stationarity, consisting of intermittent burst processes or intermittent processes. A high number of Fourier coefficients is necessary to take into account these structures which are visible on some intervals and invisible on others. Each process becomes more or less undetectable when using the classical Fourier analysis.

Wavelet analysis has been developed in order to provide a performing analysing tool for this kind of signal. It effectively renders possible a time–scale localisation of the process thanks to a projection on a class of functions which in turn makes it possible to extract information within a local neighbourhood.

1. The wavelet transform

1.1. A question of projection

Analysing a signal basically consists of looking for similarity between the signal and well-known mathematical functions usually underlined by a clear physical meaning. In mathematics, the degree of similarity between two square continuous-time integrable signals $x(t)$ and $y(t)$ can be indicated using the classical scalar product $I(x,y)$ defined as:

$$I_{XY} = \int_{-\infty}^{+\infty} x(t)y(t)\mathrm{d}t \tag{1}$$

If $I(x,y)$ is equal to zero, the two functions are said to be orthogonal. Any signal $x(t)$ can then be projected and analysed using a set of functions $y(t,\{p_i\}_{I=1,\ldots,N})$, where $\{p_i\}_{I=1,\ldots,N}$ is a set of characteristic parameters:

$$I_{XY}(p_i) = \int_{-\infty}^{+\infty} x(t)y(t,p_i)\mathrm{d}t \tag{2}$$

In a reverse manner, $x(t)$ can be expanded in terms of a linear superposition of the set of functions $y(t,\{p_i\})$. If the functions $y(t,\{p_i\})$ are orthogonal to each other, the signal $x(t)$ is then characterised by the values of the scalar product between the signal $x(t)$ and the projection basis $y(t,\{p_i\})$. It should be noted that, in general, in spreading a one-dimensional temporal or spatial signal in a n-dimensional representation, the functional representation is said to be redundant. Two well-known physical analyses are based on these properties: the Fourier transform and the Gabor transform.

The Fourier transform can be viewed as a projection of the temporal domain to the frequency domain (ω) using the set of functions:

$$y(t,\omega) = \exp(\mathrm{i}2\pi\omega t) \Rightarrow S(\omega) = \int_{-\infty}^{+\infty} x(t)y(t,\omega)\mathrm{d}t \tag{3}$$

The scalar product $S(\omega)$ is the spectral amplitude of the signal $x(t)$ at the frequency ω. It corresponds to the convolution of the signal over the trigonometric orthogonal basic defined by $\{\exp(\mathrm{i}\omega_n t), n\in(R)\}$, where ω_n is a discrete frequency ($\omega_n = 2\pi n/T$). A comprehensive review of spectral analysis can be found in Papoulis (1964), Priestley (1981), and Ghil et al. (2002). Recent application to discharge time series can be found in Pelletier and Turcotte (1997) and Tessier et al. (1996).

Another important class of projection consists in the windowed Fourier transform defined by Gabor (1946). The two parameters windowed Fourier transform noted SG is a two-parameter transform defined by

$$y(t_1,t_2,\omega) = \exp(\mathrm{i}2\pi\omega t)\Phi\left(\frac{t_1-t_2}{\sigma}\right) \Rightarrow \mathrm{SG}(\omega, t_1-t_2) = \int_{-\infty}^{+\infty} x(t)y(t_1,t_2,\omega)\mathrm{d}t \tag{4}$$

where $\Phi(t_1 - t_2/\sigma)$ is the windowed Fourier function different from zero only around t_2 on a time domain $[-\sigma/2{:}\sigma/2]$. A commonly used function is a Gaussian of width σ defined by:

$$\Phi\left(\frac{t_1-t_2}{\sigma}\right) = \exp\left(-\mathrm{i}\sigma^2\frac{(t_1-t_2)^2}{2}\right) \tag{5}$$

The wavelet transform constitutes the last type of projection that will become more developed since it constitutes the most valuable analysis when dealing with hydrological signals.

1.2. The wavelet transform in geosciences

Within the field of earth sciences, Grossman and Morlet (1984) introduced the wavelet transform for the treatment of geophysical seismic signals. A very comprehensive and pedagogical mathematical presentation of wavelet analyses can be found in Walker (1997). A review of wavelet in geosciences can be found in FoufoulaGeorgiou and Kumar (1995). This paper will concentrate on the most recent contributions in the field of earth sciences:

- Fluid mechanics with isolation of coherent structures in turbulent flows (Argoul et al., 1989; Liandrat et al., 1990; Farge and Rabreau, 1988; Farge, 1992; Long et al., 1993; Higuchi et al., 1994; Katul et al., 1994, 1995a, 1995b).
- Meteorology with temporal variability of coherent convective storm structures (Kumar and Foufoula-Georgiou, 1993; Takeuchi et al., 1994; Venugopal and Foufoula-Georgiou, 1996; Kumar, 1996), and examination of turbulence structures above forest canopy (Turner et al., 1994; Katul and Parlange, 1995a,b; Szilagi et al., 1999; Katul et al., 1998, 2001).
- Oceanography with ocean temperature variability (Meyers and O'Brien, 1994; Flinchem and Jay, 2000) and sea level fluctuations (Percival and Mofjeld, 1997).
- Climatology with long-term land temperature series (Benner, 1999; Baliunas et al., 1997), sea surface temperature fluctuations (Meyers and O'Brien, 1993), wetness indice series (Jiang et al., 1997), climate change detection (Fraedrich et al., 1997; Jung et al., 2002; Tyson et al., 2002) and climatic index variations (Torrence and Webster, 1999; Higuchi et al., 1999; Jury et al., 2002; Lu et al., 2002; Janicot et Sultan, 2000).
- Paleoclimatology with oxygen isotopic ratios from marine sediments (Bolton et al., 1995; Prokhoff and Veizer, 1999) loess sequence analysis over North China (Heslop et al., 2002).
- Geophysics with long-term geomagnetic paleointensity fluctuations (Yokoyama and Yamazaki, 2000; Guyodo et al., 2000), magnetosphere and aurora phenomenon insight (Lui, 2002).

The earlier wavelets applications to discharge time series consist of an identification and classification of the different regimes of several American catchments operated by Smith et al. (1998). Recent investigations on the application of wavelets to discharge time series should also be mentioned.

In South America, Compagnucci et al. (2000) examined the influence of ENSO over a subtropical Argentinean river using the wavelet approach which indicates variability in bands larger than 10 years. Gaucherel (2002) detected and explained the 'Short March Summer' meteorological phenomenon over the Guyana Shield using wavelet analysis of the Guyanian watershed discharge series. Labat et al. (2004) proposed a wavelet analysis of the annual rainfall over the Amazon basin and of the annual regime of the Amazon discharge at Obidos, in relationship to climatic drivers.

In North America, Lafreniere and Sharp (2003) used wavelet analysis to identify seasonal and interannual variability in temperature, precipitation and discharge of glacial and nival Canadian stream catchments. Anctil and Coulibaly (2004) and Coulibaly and Burn (2004) put in evidence 2–6 year interannual variability in the Southern Quebec stream flow.

Jury et al. (2002) also indicates using wavelet analysis to demonstrate a 2–4 year variability in Congo discharges. Finally, applications to karstic spring discharges allows for the identification of the different components of the aquifer global response, as mentioned in Labat et al. (2000, 2001).

1.3. Basics over the wavelet transform

The basic aim of wavelet analysis is both to determine the frequency (or scale) content of a signal and to assess and determine the temporal variation of this frequency content (Heil and Walnut, 1989). This property is in complete contrast to the Fourier analysis, which allows for the determination of the frequency content of a signal but fails to determine frequency time-dependence. Therefore, the wavelet transform is the tool of choice when signals are characterised by localised high frequency events or when signals are characterised by a large numbers of scale-variable processes. Because of its localisation properties in both time and scale, the wavelet transform allows for tracking the time evolution of processes at different scales in the signal.

This time–scale wavelet transformation $C_\psi^x(a,\tau)$ is defined in the case of a continuous time signal as

$$C_{\psi}^{x}(a,\tau) = \frac{1}{\sqrt{a}} \int_{-\infty}^{+\infty} x(t)\psi^{*}\left(\frac{t-\tau}{a}\right)\mathrm{d}t \quad (6)$$

where * corresponds to the conjugate. The function $\psi(t)$, which can be real or complex, plays the role of a convolution-kernel and is called a wavelet. The wavelet function must fulfil some strict mathematical conditions. For example, the time–scale localisation property requires that wavelet functions must be characterised, in both time and frequency domains, by compact supports or, at least, by a sufficiently fast decay. Mathematically, these properties can be formalised by two conditions, called 'admissibility conditions'.

The parameters a and τ are used to adjust the shape and location of the wavelets, respectively, in scale and time domains. The term $1/\sqrt{a}$ keeps the energy of the scaled-dilated wavelet equal to the energy of the initial wavelet $\psi(t)$. As the parameter a changes, the wavelet is dilated or compressed in order to cover a large interval of frequencies or scales. Changing t allows for moving the centre of the wavelet. One should note that in contrast to the windowed Fourier transform, the wavelet transform has an improved ability to 'zoom in' and 'zoom out' in order to identify the different included processes. In this sense, the wavelet transform is a sort of microscope with magnification $1/a$ and location given by the parameter τ. If the signal $x(t)$ has no significant variation at the scale of $\psi_a(t)$ in the vicinity of a signal at time t_0, the wavelet coefficient is near zero. Conversely, if $x(t)$ evolves around a given point t_0 and at a given scale a_0, the corresponding coefficient is large in the vicinity of the point (t_0,a_0).

The results of the wavelet analysis of a signal is highly correlated to the choice of the wavelet. Particular attention, therefore, should be paid to wavelet determination. The Morlet wavelet, first introduced by Morlet, is used here

$$\psi(t) = \exp(-\mathrm{i}\omega_0 t)\exp(-t^2/2) \quad (7)$$

which implies that its Fourier transform $\hat{\psi}(\omega)$ is defined by:

$$\hat{\psi}(\omega) = \exp(-(\omega-\omega_0)^2/2) \quad (8)$$

Because of its Gaussian envelop, the Morlet wavelet achieves the optimum of localisation in real and Fourier spaces as shown by Heisenberg's uncertainty theorem. The Heisenberg inequality states that there is a lower limit to the product of frequency and time resolution. As time resolution is improved, frequency resolution degrades. Similarly, when frequency resolution is increased, temporal resolution degrades.

Once the analysis step is completed, the next step is the isolation of relevant sub-scale processes. The synthesis of the continuous time signal $x(t)$ through its wavelet coefficients $C_X(a,\tau)$ can be achieved using the reconstruction formula:

$$x(t) = \frac{1}{K_{\psi}} \int_{0}^{+\infty} \int_{-\infty}^{+\infty} C_x(a,\tau)\psi_{a,\tau}(t)\frac{\mathrm{d}a\mathrm{d}\tau}{a^2} \quad (9)$$

The integration over the whole scale interval allows for the reconstruction of the signal. The integration over a restricted scale interval $[a_1,a_2]$ allows for the isolation and identification of the processes with characteristic scale comprises between a_1 and a_2.

In hydrology a continuous time signal process is not always available. More often, there is a discrete-time signal, which will be denoted by $x(i)$. The orthogonal discrete wavelet transform coefficients $C_{j,k}$ are then defined by analogy with the continuous wavelet transform (Daubechies, 1990, 1992; Jawerth and Sweldens, 1994; Strang, 1989)

$$C_{j,k}^{x} = \int_{-\infty}^{+\infty} x(t)\psi^{*}(t)\mathrm{d}t \quad \text{with} \quad \psi_{j,k}(t) = 2^{j/2}\psi(2^j t - k) \quad (10)$$

where * corresponds to the complex conjugate and $(k,j)\in Z^2$. The integer j is the scale factor, analogous to the a parameter and the integer k is the translation factor analogous to the τ parameter. This constitutes the conceptual basis of multiresolution analysis. Multiresolution wavelet analysis (Mallat, 1989) allows for the decomposition of a function or a signal in a progression of successive 'approximations' and 'details', corresponding to different scales j. In the companion paper, a original combined multiresolution-continuous wavelet analysis is proposed.

1.4. Some applications on synthetic signals

As previously mentioned, the main property of the wavelet transform is to make possible a time–scale discrepancy of processes. Several applications of continuous wavelet transformation to synthetic signals are exposed (Fig. 1).

Two free Matlab-softwares are used to obtain the results of the practical study. The first one is provided by the University of Vigo (Uvi-Wave 3.0) and is available at the URL: ftp.tsc.uvigo.es with a download user manual (Gonzales et al., 1996); the second one was kindly provided by Torrence and Campo (1998) at the URL http://paos.colorado.edu/research/wavelets/.

The two first signals (1a and 1b) propose a simple, but representative confrontation of the Fourier and continuous wavelet transforms. They are both constituted of two sinusoidal functions characterised by a single frequency. On the first signal, both frequencies occur during the whole interval of observation, and on the second, they are temporally localised, respectively, on the first and second halves of the time interval. The two Fourier spectra appear as being very similar, whereas wavelet coefficients clearly exhibit the temporal discrepancy of the two components. High wavelet coefficients corresponding to the two scales (lighter color) are visible on the whole interval for the first signal. For the second signal, two temporally localised bands are clearly distinguishable. These correspond to the two different sub-process scales.

The third signal (1c) illustrates a temporal variation of the characteristic frequency. This signal is composed of a cosine with a characteristic frequency varying in time within a power law. Fourier spectra highlights a plateau with no evident characteristic frequency, whereas continuous Morlet wavelet spectrum exhibits a parabolic variation of the characteristic frequency with time.

2. Thermodynamics indicators in wavelet analysis

The main issue with hydrological and climatic time series consists of the presence of several processes occurring over a large scale interval. We see that the continuous orthogonal wavelet analyses are the tool of choice in treating these signals. This analysis should be completed, however, by using new indicators recently introduced in wavelet analyses.

More performing indicators based on thermodynamics concepts such as energy or entropy could be introduced in order to confirm or highlight the underlying dynamics of the hydrological system.

2.1. Energy repartition in the wavelet frame

The repartition of energy in the signal allows for the determination of the scales which concentrate the essential dynamic of a signal. Therefore, a determination of the temporal variations of the distribution of energy across the scales is an important application of the wavelet transform.

Previously, the Fourier transform allowed for the determination of the distribution of energy across frequencies ω using the Power spectrum density $P_{XX}(\omega)$ defined for a signal $x(t)$ by:

$$P_{XX}(\omega) = \left| \frac{1}{T} \int_0^T x(t)^2 \exp(-i2\pi\omega t)\mathrm{d}t \right|^2 \tag{11}$$

The companion concept of wavelet energy was first defined by Hudgins et al. (1993) and Brunet and Collineau (1995). Other results concerning wavelet variance estimators and applications can be found in Percival (1995), Percival and Mofjeld (1997), Poggie and Smits (1997), Li and Nozaki (1997), and Onorato et al. (1997).

This concept is based on the conservation of energy between the time domain and the time–scale domain, i.e.:

$$\int_{-\infty}^{+\infty} x^2(t)\mathrm{d}t = \frac{1}{K_\psi} \int_0^{+\infty} \int_{-\infty}^{+\infty} |C_x(a,\tau)|^2 \frac{\mathrm{d}a\mathrm{d}\tau}{a^2} \tag{12}$$

Therefore, the total signal variance can be distributed in the wavelet domain and the wavelet spectrum $W_X(a,\tau)$ of a continuous-time signal $x(t)$ which can be defined, by analogy with the Fourier analysis, as the modulus of its wavelet coefficients (Liu, 1995):

$$W_X(a,\tau) = C_X(a,\tau)C_X^*(a,\tau) = |C_X(a,\tau)|^2 \tag{13}$$

According to Meneveau (1991), the concept of wavelet variance can be defined by using the orthogonal multiresolution approach. The total energy (variance) $T_X(m)$ captured by the detail D_m at scale m of a signal $x(i)$ of length 2^M can be estimated as

$$T_x(m) = \frac{1}{2^{M-m}} \sum_{j=1}^{2^{M-m}} (D_{m,j}^x)^2 \tag{14}$$

where $D_{m,j}$ is defined as in Eq. (11). Note that these concepts were first implemented to study intermittent turbulent signal above the forest canopy (Turner et al., 1994; Katul et al., 1994, 1995).

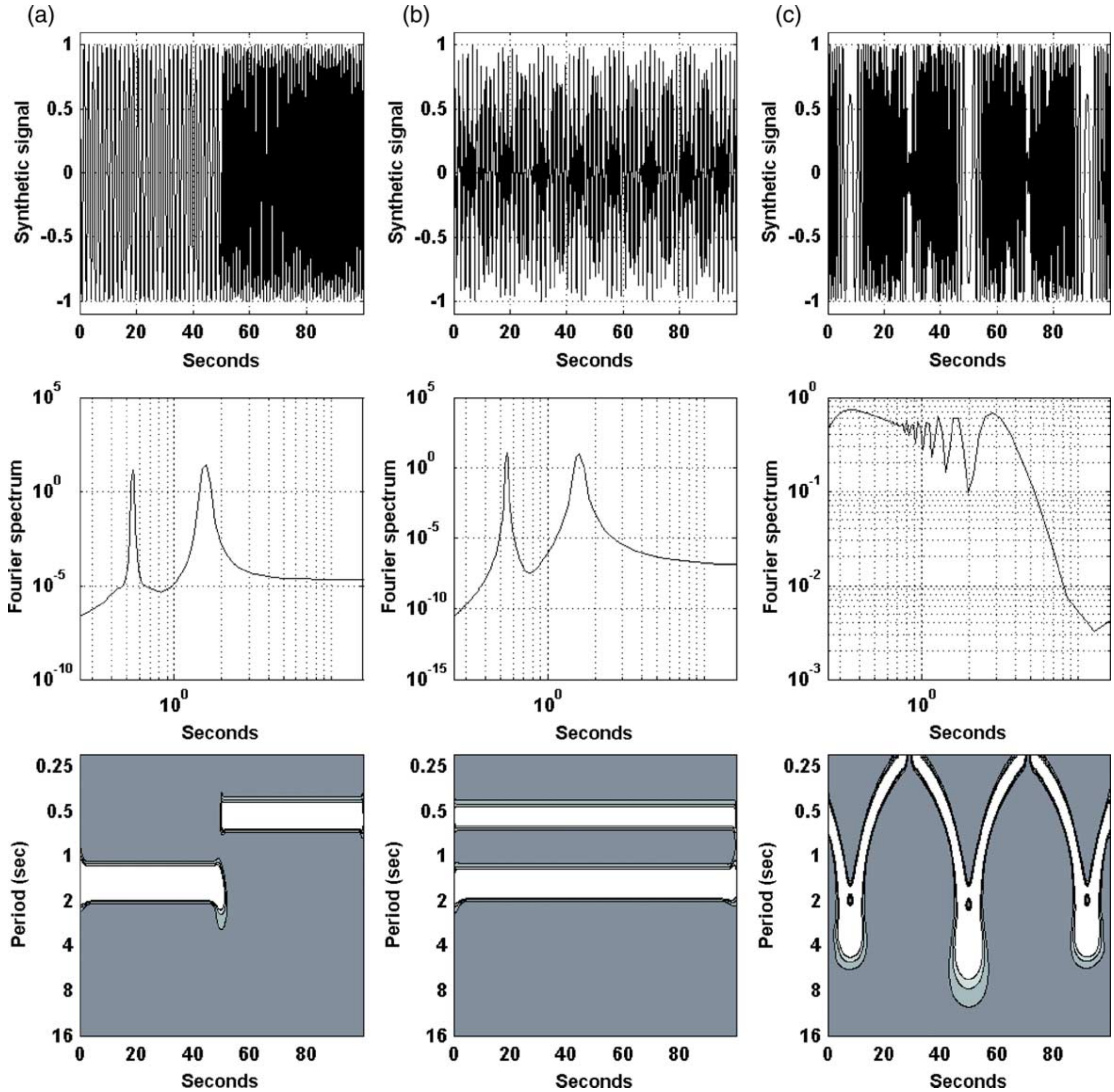

Fig. 1. Illustration and confrontation of Fourier and continuous wavelet transform on synthetic signals. (a and b) Signals composed of two frequencies presented at overlapped and non-overlapped time intervals (top). Both signals exhibit similar spectral densities (middle) despite their significantly different temporal signatures. However, continuous Morlet wavelet spectra (bottom) display the time localization of the two different sub-processes. (c) Signal composed of a cosine with a characteristic frequency varying in time within a parabolic law (top), named 'chirp'. Fourier spectra (middle) highlight a plateau with no evident characteristic frequency. Continuous Morlet wavelet spectrum exhibits the parabolic temporal variation of the characteristic frequency. (d) Signal composed of cosine function multiplied by an exponential function (top). Fourier spectrum (middle) exhibits the characteristic frequency but in a similar way to that of an un-localized periodic function. [*color code:* the lighter the color, the higher the coefficient.]

2.2. Entropy in the wavelet frame

The second important thermodynamic concept consists in entropy. Entropy is a measure of the degree of uncertainty, i.e. of the chaos or of the lack of information in a system characterised by a time series (Bates, 1993). Note that the entropy concept has already been used in hydrology, especially in basin geomorphology and water resource management (Singh, 2000).

If complete information is available on a system, its entropy will be equal to zero. If some uncertainty remains, it will be greater than zero. In considering a set composed of n events, uncertainty consists in the determination of which event will occur. This uncertainty can be qualified using two factors: the number of possible events and the probability distribution of the events.

The first definition of entropy is proposed by S Shannon (1946) as

$$S = H_1 = -\sum_{i=1}^{N} p_i \ln(p_i) \tag{15}$$

with the convention $0 \ln 0 = 0$ by definition. This equation makes it possible to quantify the general disorder of a system, including all the values present in the system (in this instance, the hydrological or climatic system). Shannon (1946) introduced the entropy S, defined in Eq. (14), in order to interpret the thermodynamic concept of entropy in terms of information content. Maximum Shannon entropy is equal to $\ln(N)$, where N is the number of classes of the density probability distribution.

Shannon entropy S can also be defined in a continuous framework:

$$S = \int_0^{\infty} -f(x)\ln(f(x))\mathrm{d}x \tag{16}$$

where $f(x)$ is the continuous density probability function of the variable x.

Given a frequency distribution of a dataset noted $\{p_i\}$, Rényi (1976) also defined as generalised entropy noted H_α

$$H_\alpha = \frac{1}{1-\alpha}\mathrm{Ln}\left(\sum_{i=1}^{N} p_i^{\alpha}\right) \tag{17}$$

where α is a parameter. Note that the special case corresponding to $\alpha = 1$ corresponds to Shannon entropy.

However, probability distribution is not the only kind of distribution which can give information. This definition has also been extended to other types of distributions. This paper will focus on the extension of Shannon entropy to energy distribution.

Using a Fourier energy distribution, a new frequency distribution (FD) entropy noted S_{FD}

$$S_{\mathrm{FD}}(\omega) = \int_0^{\infty} -P_{\mathrm{XX}}(\omega)\ln(P_{\mathrm{XX}}(\omega))\mathrm{d}x \tag{18}$$

can be defined where $P_{XX}(\omega)$ is the Fourier spectrum of the variable x. This Fourier-based entropy has already been applied in hydrology by Sonuga (1976). In a similar way, this generalisation can also be achieved considering time–frequency distributions. Considering, for example, a time frequency energy representation from Cohen's class $C(t,\omega)$ defined as

$$C(t,\omega) = \frac{1}{4\pi^2}\iiint \phi(\theta,\tau)x\left(u+\frac{\tau}{2}\right)x\left(u-\frac{\tau}{2}\right) \times \exp(\mathrm{i}(\theta u - \theta t - \omega\tau))\mathrm{d}u\mathrm{d}\theta\mathrm{d}\tau \tag{19}$$

the time frequency distribution (TFD) entropy S_{TFD} can be defined as:

$$S_{\mathrm{TFD}}(t,\omega) = \int_0^{\infty} -|C_x(t,\omega)|^2\ln(|C_x(t,\omega)|^2)\mathrm{d}t\mathrm{d}\omega$$

This formulation is interesting as it allows for a temporal evolution of the disorder of a system.

Since Shannon entropy constitutes a useful criterion for analysing system's order or disorder using any energy probability density function distribution, a time–scale distribution called wavelet entropy can be introduced. A large majority of these concepts have been recently and successfully developed and applied in neurosciences (Lemire et al., 2000; Wessel et al., 2000; Quiroga et al., 2001; Rosso and Mairal, 2002; Yordanova et al., 2002; Rosso et al., 2003).

The continuous wavelet entropy noted S_{W} defined as (Sello, 2003)

$$S_{\mathrm{W}}(t) = \int_0^{\infty} -P_{\mathrm{W}}(a,t)\ln(P_{\mathrm{W}}(a,t))\mathrm{d}a \tag{20}$$

where

$$P_{\mathrm{W}}(a,t) = \frac{|W_\psi^x(a,\tau)|^2}{\int |W_\psi^x(a,\tau)|^2\mathrm{d}a}$$

corresponds to the wavelet energy probability distribution for each scale a at time t.

Wavelet entropy is minimum when the signal is characterised by an ordered activity and wavelet entropy is maximum when the signal consists of a superimposition of large number processes (or 'of a large number of processes'). Namely, when considering an ordered mono frequency signal, a wavelet multiresolution or continuous wavelet representation of such a signal is resolved around one unique scale or level. This particular level then concentrates around 100% of the total energy of the signal. The wavelet entropy then will be near to zero. When considering a signal generated by a white noise, for example, all levels will carry a certain amount of energy. These levels can also be expected to carry the same level of energy and, consequently, the wavelet entropy will be maximal.

Through this multiscale approach, relevant scale levels can automatically be detected which include the main complex processes of the system.

A multiresolution wavelet entropy can also be defined, allowing for a scale representation of the disorder of a system (Blanco et al., 1998). Once the multiresolution coefficients $C_{XX}(j,k)$ have been calculated using Eq. (10), the energy at time k and for scale j, $E(j,k)$ can be approximated by $E(j,k)=|C_{XX}(j,k)|^2$. As previously seen, summing this energy for all discrete time k leads to an approximation of the energy content at scale j noted $E(j)$

$$E(j) = \frac{1}{N}\sum_k E(j,k) \tag{21}$$

In order to follow the Shannon entropy framework, a probability density function must be defined as the ration between the energy of each level and total energy:

$$p_E(j) = \frac{E(j)}{\sum_j E(j)} \tag{22}$$

This corresponds exactly to the probability density distribution of energy across the scales. It must also be noted that, because of the orthogonal representation, the following relation holds:

$$\sum_j p_E(j) = 1 \tag{23}$$

Finally, the multiresolution wavelet SMR(j) entropy at the scale j is defined by analogy with the continuous wavelet entropy:

$$\mathrm{SMR}(j) = -p_E(j)\ln(p_E(j)) \tag{24}$$

The temporal evolution of multiresolution wavelet entropy is achieved by decomposing the signal and calculating on these intervals the entropy as defined above.

3. New insights in the time–scale relationship between two signals

In the previous sections, the importance of the introduction of wavelet energy and wavelet entropy to characterise the degree of complexity of a signal was noted. In this part, attention will be given to the introduction of wavelet indicators to investigate the relationship between two given signals, e.g. rainfall rates/discharges and discharge/climate circulation indexes.

3.1. Wavelet cross-correlation

In the same manner as in Fourier analyses, wavelet cross-correlation should sometimes be preferred to classical cross-correlation. This method effectively provides new insights into the scale dependant degree of correlation between two given signals (Onorato et al., 1997; Labat et al., 2002).

Classical cross-correlation makes it possible to quantify the degree of similarity between two signals notes $x(t)$ and $y(t)$. The cross-correlation R_{XY} between two stochastic process is defined as

$$R_{XY} = \frac{C_{XY}}{\sqrt{C_{XX}C_{YY}}} \tag{25}$$

with $C_{XY}=E[x(t)y(t)]$, $C_{XX}=E[x(t)^2]$, $C_{YY}=E[y(t)^2]$.

It is to be recalled that under stationary and ergodic assumptions

$$E[x(t)y(t)] = \lim_{T\to\infty}\frac{1}{T}\int x(u)y(u)\mathrm{d}u$$

This notion has been generalised in order to introduce a time delay between two signals:

$$R_{XY}(t_1-t_2) = \frac{C_{XY}(t_1-t_2)}{\sqrt{C_{XX}(0)C_{YY}(0)}} \quad \text{with} \quad C_{XY}(t_1-t_2) = E[X(t-t_1)Y(t-t_2)] \tag{26}$$

Eq. (26) clearly indicates that cross-correlation analysis provides a quantitative measure of the relatedness of two signals, shifting in time with respect to each other. It allows for the identification of common components occurring at the same delay.

However, if the signals include non-stationary components, the cross-correlation becomes invalid. The same conclusion arises if both signals are characterised by highly variable processes occurring over a wide range of scales.

In answer, the continuous wavelet cross-correlation is introduced which overcomes the limitations of classical correlations.

Considering two correlated processes $x(t)$ and $y(t)$, the wavelet cross-correlation function noted $WC_{XY}(a,u)$ for a given scale a and a given time delay u can be defined as (Li and Nozaki, 1997):

$$\mathrm{WC}_{XY}(a,u) = E[W_{XX}(a,\tau)W_{YY}(a,\tau+u)] \tag{27}$$

At this point, some authors recommend distinguishing the real part noted $\mathrm{RWC}_{XY}(a,\tau)$ from the imaginary part $\mathrm{IWC}_{XY}(a,\tau)$ of the wavelet cross-correlation (REF), arguing that the real part alone is sufficient to quantify the strength of correlation between both signals at a given scale a. The wavelet cross-correlation is then defined by:

$$\mathrm{WR}_{XY}(a,u) = \frac{\mathrm{RWC}_{XY}(a,u)}{\sqrt{\mathrm{RWC}_{XX}(a,0)\mathrm{RWC}_{YY}(a,0)}} \tag{28}$$

Sello and Bellazzini (2000) propose to consider only the real part of the wavelet transform and define a wavelet local correlation coefficient WLCC (a,u) based on the wavelet cross-spectrum $W_{XY}(a,u) = W^*_{XX}(a,u)W_{YY}(a,u)$ and defined as

$$\mathrm{WLCC}(a,u) = \frac{\mathrm{Real}(W_{XY}(a,u))}{|W_{XX}(a,u)||W_{YY}(a,u)|} \tag{29}$$

This wavelet local correlation coefficient WLCC (a,u) definition is based on the following relationship between the classical cross-correlation and the real part of the cross-wavelet-spectrum:

$$\int_{-\infty}^{+\infty} x(t)y(t)\mathrm{d}t = \frac{1}{C_\psi}\int_0^{+\infty}\int_{-\infty}^{+\infty} \mathrm{Real}(W_{\mathrm{XY}}(a,\tau))\mathrm{d}a\mathrm{d}\tau \tag{30}$$

However, real part and imaginary part wavelet analysis ( ) does not provide clear separate information. As in the Fourier analysis, only modulus and arguments will be considered here as interpretative. This conclusion is confirmed by Mizuno-Matsumoto et al. (2001, 2002) who noted in a preliminary analysis no significant differences between the definitions. Wavelet cross-correlation is then defined as

$$\mathrm{WR}_{XY}(a,\tau) = \frac{\sqrt{|\mathrm{RWC}_{XY}(a,\tau)|^2 + |\mathrm{IWC}_{XY}(a,\tau)|^2}}{\sqrt{|\mathrm{WC}_{XX}(a,0)||\mathrm{WC}_{YY}(a,0)|}} \tag{31}$$

where RWC_{XY} and IWC_{XY} are, respectively, the real and imaginary part of the cross-wavelet correlation function defined by Eq. (27).

An illustration of the wavelet cross-correlation on multiscale synthetic signals is depicted in Fig. 2. The first signal (thin line) corresponds to $y_1(t) = \sin(40t)\exp(-(t-5)^2) + \sin(20t)\exp(-(t-5)^2) + \sin(10t)\exp(-(t-5)^2)$. The second signal (dark line) corresponds to $y_2\,(t) = \sin(40(t-3))\exp(-(t-8)^2) + \sin(20(t-2))\exp(-(t-7)^2) + \sin(10(t-1))\exp(-(t-6)^2)$. The three scale processes are then, respectively, delayed by a 3, 2 and 1 s. The wavelet cross-correlation allows a rapid and efficient time–scale identification of these delays.

In conclusion, the introduction of wavelet cross-correlation allows a rapid identification of the degree of correlation between processes at a given scale and the determination of the delay between these processes.

3.2. Wavelet coherence

The notion of coherence in signal processing consists, from a general point of view, of a measure of the correlation between two signals or between two representations of these signals. In examining two continuous finite-energy signals $x(t)$ and $y(t)$, the classical cross-correlation already defined in the previous section can be considered as a temporal coherence between two signals. Given the Fourier transform of these signals, the spectral coherence can be defined (Gardner, 1992) as

$$\rho(f) = \frac{|S_{XY}(f)|}{\sqrt{|S_{XX}(f)S_{YY}(f)|}} \tag{32}$$

where $S_{XY}(f)$ is the cross-spectral density between the two processes $x(t)$ and $y(t)$. One recalls that under stationary and ergodic assumptions, the cross-Fourier spectrum is defined as:

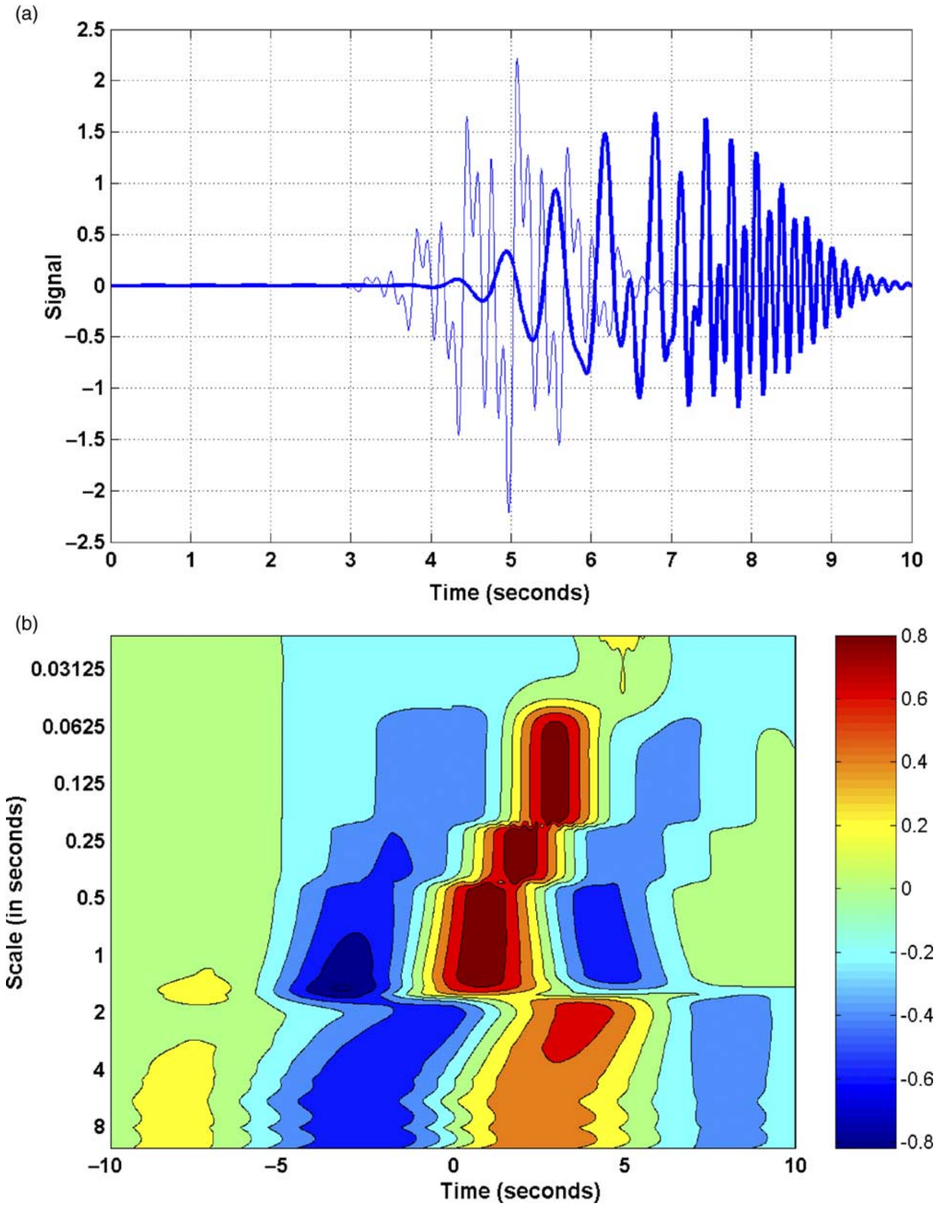

Fig. 2. Illustration of the wavelet cross-correlation on multiscale synthetic signals. The first signal (thin line) corresponds to $y_1(t)=\sin(40t)\exp(-(t-5)^2)+\sin(20t)\exp(-(t-5)^2)+\sin(10t)\exp(-(t-5)^2)$. The second signal (dashed line) corresponds to $y_2(t)=\sin(40(t-3))\exp(-(t-8)^2)+\sin(20(t-2))\exp(-(t-7)^2)+\sin(10(t-1))\exp(-(t-6)^2)$. Then, the three scale processes (with periods, respectively, equal to 0.6, 0.3 and 0.08 s) are, respectively, delayed by a 3, 2 and 1 s (a). The wavelet cross-correlation (b) allows a rapid and efficient time–scale identification of these delays.

$$S_{XY}(f) = \int_{-\infty}^{+\infty} R_{XY}(\tau)\exp(-i2\pi f\tau)d\tau \qquad (33)$$

Because of the Schwartz inequality, one can note that $\rho(f)$ takes value between 0 and 1. If $\rho(f)$ is close to 1 for all frequencies, then $y(t)$ can be approximated as a linear time invariant transformation of $x(t)$.

In these definitions, the stationary assumption appears as being highly restrictive. However, when dealing with non-stationary processes, as in hydrology the use of a time–frequency representation of the signals is suggested. Such coherence highlights the temporal variations of the correlation between two signals and allows for the detection of transient high covariance. To overcome the problem inherent to non-stationary signals, it has been proposed to introduce the wavelet coherence (Torrence and Webster, 1999; Lachaux et al., 2002). The main issue is that an application of an analogue formula to Eq. (32) leads to a coherence equal to 1 for all time and scales as previously mentioned by Labat et al. (2001). Attempts have been made to avoid this problem. They essentially differ on two points: the fundamental definition of wavelet coherence and the estimation of the wavelet cross-spectrum.

On one hand, Sello and Bellazzini (2000) introduce the cross-wavelet coherence, defined as

$$\mathrm{CWCF}(a,\tau) = \frac{2|W_{XY}(a,\tau)|^2}{|W_{XX}(a,\tau)|^4 + |W_{YY}(a,\tau)|^4} \tag{34}$$

which measures the intensity coherence of the signals. However, this definition is too distant from the original Fourier formulation. On the other hand, Torrence and Webster (1999) propose to determine wavelet coherence using a smooth estimate of the wavelet spectrum and to define a smooth wavelet spectrum and cross-spectrum, respectively, noted $\mathrm{SW}_{XX}(a,\tau)$ and $\mathrm{SW}_{XY}(a,\tau)$

$$\mathrm{SW}_{XX}(a,\tau) = \int_{t-\delta/2}^{t+\delta/2} W_{XX}^*(a,\tau) W_{XX}(a,\tau)\,\mathrm{d}a\,\mathrm{d}\tau \tag{35}$$

$$\mathrm{SW}_{XY}(a,\tau) = \int_{t-\delta/2}^{t+\delta/2} W_{XX}^*(a,\tau) W_{YY}(a,\tau)\,\mathrm{d}a\,\mathrm{d}\tau \tag{36}$$

The scalar δ represents the size of the two-dimensional filter (Lachaux et al., 2002). It constitutes an important parameter of the wavelet coherence and must be adequately determined for an acceptable estimation of the wavelet coherence. The wavelet coherence can then be defined by analogy with Fourier coherence as:

$$\mathrm{WC}(a,\tau) = \frac{|\mathrm{SW}_{XY}(a,\tau)|}{\sqrt{[|\mathrm{SW}_{XX}(a,\tau)||\mathrm{SW}_{YY}(a,\tau)|]}} \tag{37}$$

One can note that the Schwarz inequality still ensures that WC takes value between 0 and 1.

4. Conclusion

This contribution provides a review of the most recent wavelet applications in the field of earth sciences. Focusing more particularly on the use of wavelet analysis on long-term discharge series, it unfortunately appears that this technique remains unknown by a large majority of land surface hydrologists, whereas it clearly overcomes the well-known limits of the classical Fourier analysis. New wavelet-based tools are proposed to hydrologists in order to make the wavelet analysis more powerful and attractive.

From a basic analysis point of view, a combined multiresolution-continuous wavelet analysis method sensitively improves the determination of the temporal variations allowing for a strict isolation of the predominant multiscale processes and a quantitative evaluation of their temporal fluctuations. The notion of wavelet entropy is introduced in order to characterise the time–scale complexity evolution of a signal. Wavelet entropy also allows the determination of the relevant scale of the signal complexity. Finally, new insights in the scale-dependence of the relationship between two signals are also proposed, with special emphasis on wavelet cross-correlation and on wavelet coherence. In conclusion, a complete review of concepts in both univariate and covariate wavelet analysis is presented. These methods will now be applied to several large river runoffs and to two global climatic indexes.

References

Anctil, F., Coulibaly, P., 2004. Wavelet analysis of the interannual variability in Southern Quebec streamflow. Journal of Climate 17 (1), 163–173.

Argoul, F., Arnéodo, G., Grasseau, G., Gagne, Y., Hopfinger, E.J., Frish, U., 1989. Wavelet analysis of turbulence reveals the multifractal nature of the Richardson cascade. Nature 338, 51–53.

Baliunas, S., Frick, P., Sokoloff, D., Soon, W., 1997. Time scales and trends in the central England temperature data (1659–1990): a wavelet analysis. Geophysical Research Letters 24, 1351–1354.

Bates, J.E., Shepard, H.K., 1993. Measuring complexity using information fluctuation. Physics Letters A 172, 416–425.

Benner, T., 1999. Central England temperatures: long term variability and teleconnections. International Journal of Climatology 19, 391–403.

Blanco, S., Figliola, A., Quiroga, R.Q., Rosso, O.A., Serrano, E., 1998. Time–frequency analysis of electroencephalogram series. III. Wavelet packets and information cost function. Physical Review E 57 (1), 932–940.

Bolton, E.W., Maasch, K.A., Lilly, J.M., 1995. A wavelet analysis of Plio Pleistocene climate indicators: a new view of periodicity evolution. Geophysical Research Letters 22 (20), 2753–2756.

Brunet, Y., Collineau, S., 1995. Wavelet analysis of diurnal and nocturnal turbulence above a maize crop. In: Foufoula-Georgiou, E., Kumar, P. (Eds.), Wavelets in Geophysics. Academic Press, New York, pp. 129–150.

Compagnucci, R.H., Blanco, S.A., Figliola, M.A., Jacovkis, P.M., 2000. Variability in subtropical Andean Argentinean Atuel river: a wavelet approach. Environmetrics 11, 251–269.

Coulibaly, P., Burn, D.H., 2004. Wavelet analysis of variability in annual Canadian streamflows. Water Resource Research 40 (3), W03105.

Daubechies, I., 1990. The wavelet transform, time–frequency localization and signal analysis. IEEE Transactions on Information Theory 36 (5), 961–1005.

Daubechies, I., 1992. Ten lectures on Wavelets. CSBM-NSF Series Appl. Math., No. 61, SIAM Publication, 357pp.

de Lima, M.I.P., Grasman, J., 1999. Multifractal analysis of 15-min and daily rainfall from a semi-arid region in Portugal. Journal of Hydrology 220, 1–11.

Farge, M., 1992. Wavelet transforms and their applications to turbulence. Annual Review of Fluid Dynamics 24, 395–457.

Farge, M., Rabreau, G., 1998. Transformée en ondelettes pour détecter et analyser les structures cohérentes dans les écoulements turbulents bidimensionnels. Comptes Rendus Academic Science Paris (II) 307, 1479–1486.

Flinchem, E.P., Jay, D.A., 2000. An introduction to wavelet transform tidal analysis methods. Estuarine, Coastal and Shelf Science 51, 177–200.

Foufoula-Georgiou, E., Kumar, P. (Eds.), 1995. Wavelets in Geophysics. Academic Press, New York, p. 337.

Fraedrich, K., Jiang, J., Gerstengarbe, F.-W., Werner, P.C., 1997. Multiscale detection of abrupt climate changes: application to Nile river flood levels. International Journal of Climatology 17, 1301–1315.

Gabor, D., 1946. Theory of communication. Journal of Institute of Electronics Engineering (London) 93 (III), 429–457.

Gardner, W.A., 1992. A unifying view of coherence in signal processing. Signal Processing 29, 113–140.

Gaucherel, C., 2002. Use of wavelet transform for temporal characterisation of remote watersheds. Journal of Hydrology 269 (3-4), 101–121.

Ghil, M., Allen, M.R., Dettinger, M.D., Ide, K., Kondrashov, D., Mann, M.E., Robertson, A.W., Saunders, A., Tian, Y., Varadi, F., Yiou, P., 2002. Advanced spectral methods for climatic time series. Review of Geophysics 40 (1), 1–41.

Gonzales, S.S., Gonzales, P.N., Garcia, G.S., 1996. Uvi-wave Wavelet Toolbox for Use with Matlab. Department of Communication Technology, University of Vigo, p. 196.

Grosmann, A., Morlet, J., 1984. Decomposition of hardy functions into square integrable wavelets of constant shape. SIAM Journal of Mathematical Analysis, 723–736.

Guyodo, Y., Gaillot, P., Channell, J.E.T., 2000. Wavelet analysis of relative geomagnetic paleointensity at ODP Site 983. Earth and Planetary Science Letters 184, 109–123.

Heil, C.E., Walnut, D.F., 1989. Continuous and discrete wavelet transforms. SIAM Review 31 (4), 628–666.

Heslop, D., Dekkers, M.J., Langereis, C.G., 2002. Timing and structure of the mid-pleistocene transition: records from the loess deposits of northern China. Palaeogeography, Palaeoclimatology, Palaeoecology 2880, 1–11.

Higuchi, H., Lewalle, J., Crane, P., 1994. On the structure of a two-dimensional wake behind a pair of flat plates. Physics of Fluids 6 (1), 297–305.

Hudgins, L., Friehe, C.A., Mayer, M.E., 1993. Wavelet transforms and atmospheric turbulence. Physical Review Letters 71 (20), 3279–3282.

Janicot, S., Sultan, B., 2000. Intra-seasonal modulation of convection in the West African monsoon. Geophysical Research Letters 28 (2), 523–526.

Jawerth, B., Sweldens, W., 1994. An overview of wavelet based multiresolution analyses. SIAM Review 36 (3), 377–412.

Jiang, J., Zhang, D., Fraedrich, K., 1997. Historic climate variability of wetness in east China (960–1992): a wavelet analysis. International Journal of Climatology 17, 969–981.

Jung, H.-S., Choi, Y., Lim, G.-H., 2002. Recent trends in temperature and precipitation over South Korea. International Journal of Climatology 22, 1327–1337.

Jury, M.R., Enfield, D.B., Mélice, J.L., 2002. Tropical monsoons around Africa: stability of El Nino-Southern oscillation associations and links with continental climate. Journal of Geophysical Research 107. 2000JC000507.

Katul, G.G., Parlange, M.B., 1995a. Analysis of land surface heat fluxes using the orthonormal wavelet approach. Water Resources Research 31 (11), 2743–2749.

Katul, G.G., Parlange, M.B., 1995b. The spatial structure of turbulence at production wavenumbers using orthonormal wavelets. Boundary Layer Meteorology 75, 81–108.

Katul, G.G., Parlange, M.B., Chu, C.R., 1994. Intermittency, local isotropy, and non-gaussian statistics in atmospheric surface layer turbulence. Physics of Fluids 6 (7), 2480–2492.

Katul, G.G., Schieldge, J., Hsieh, C.-I., Vidakovic, B., 1998. Skin temperature perturbations induced by surface layer turbulence above a grass surface. Water Resource research 34 (5), 1265–1274.

Katul, G., Lai, C.-T., Schäfer, K., Vidakovic, B., Albertson, J., Ellsworth, D., Oren, R., 2001. Multiscale analysis of vegetation surface fluxes: from second to years. Advances in Water Resources 24, 1119–1132.

Kumar, P., 1996. Role of coherent structure in the stochastic dynamic variability of precipitation. Journal of Geophysics Research 101 (26), 393–404.

Kumar, P., Foufoula-Georgiou, E., 1993. A multicomponent decomposition of spatial rainfall fields. Segregation of large and small scale features using wavelet transform. Water Resources Research 29 (8), 2515–2532.

Labat, D., Ababou, R., Mangin, A., 2000. Rainfall–runoff relations for karstic springs. Part II: Continuous wavelet and discrete orthogonal multiresolution analyses. Journal of Hydrology 238, 149–178.

Labat, D., Ababou, R., Mangin, A., 2001. Introduction of wavelet analyses to rainfall/runoffs relationships for a karstic basin: the case of Licq-Atherey karstic system (France). Ground Water 39 (4), 605–615.

Labat, D., Ababou, R., Mangin, A., 2002. Analyse multirésolution croisée de pluies et débits de sources karstiques. Comptes Rendus de l'Académie des Sciences de Paris, Géosciences 334, 551–556.

Labat, D., Ronchail, J., Callede, J., Guyot, J.L., De Oliveria, E., Guimarães, W., 2004. Wavelet analysis of Amazon hydrological regime variability. Geophysical Research Letter 31, L02501.

Lachaux, J.P., Lutz, A., Rudrauf, D., Cosmelli, D., Le Van Quyen, M., Martinerie, J., Varela, F., 2002. Estimating the time-course of coherence between single trial brain signals: an introduction to wavelet coherence. Neurophysiology Clinic 32, 157–174.

Lafreniere, M., Sharp, M., 2003. Wavelet analysis of inter-annual variability in the runoff regimes of glacial and nival stream catchments, Bow Lake, Alberta. Hydrological Processes 17 (6), 1093–1118.

Lemire, D., Pharand, C., Rajaonah, J.-C.R., Dubé, B., LeBlanc, A.-R., 2000. Wavelet time entropy, T wave morphology and myocardial ischemia. IEEE Transactions in Biomedical Engineering 47 (2), 1–11.

Li, H., Nozaki, T., 1997. Application of wavelet cross-correlation analysis to a plane turbulent jet. JSME International Journal, Series B 40 (1), 58–66.

Liandrat, J., Moret-Bailly, F., 1990. The wavelet transform: some applications to fluid dynamics and turbulence. European Journal of Mechanics B 9 (1), 1–19.

Liu, P.C., 1995. Wavelet spectrum analysis and ocean wind waves. In: Foufoula-Georgiou, E., Kumar, P. (Eds.), Wavelets in Geophysics. Academic Press, New York, pp. 151–166.

Long, S.R., Lai, R.J., Huang, N.E., Spedding, G.R., 1993. Blocking and trapping of waves in an inhomogeneous flow. Dynamics of Atmospheres and Oceans 20, 79–106.

Lu, H., Zhang, F., Liu, X., 2002. Patterns and frequencies of the East Asian winter monsoon variations during the past million years revealed by wavelet and spectral analyses. Global and Planetary Change 35, 67–74.

Lui, A.T.Y., 2002. Multiscale phenomena in the near-Earth magnetosphere. Journal of Atmospheric and Solar-Terrestrial Physics 64, 125–143.

Mallat, S., 1989. A theory for multiresolution signal decomposition: the wavelet representation. IEEE Transactions on Pattern Analysis and Machine Intelligency 11, 674–693.

Mandelbrot, B.B., Wallis, J.R., 1968. Noah, Joseph and operational hydrology. Water Resources Research 4 (5), 909–918.

Meneveau, C., 1991. Analysis of turbulence in the orthonormal wavelet representation. Journal of Fluid Mechanics 232, 469–520.

Meyers, S.D., O'Brien, J.J., 1994. Spatial and temporal 26-day SST variations in the equatorial Indian ocean using wavelet analysis. Geophysical Research Letters 21 (9), 777–780.

Meyers, S.D., Kelly, B.G., O'Brien, J.J., 1993. An introduction to wavelet analysis in oceanography and meteorology with application to the dispersion of Yanai waves. Monthly Weather Reviews 121 (10), 2858–2866.

Mizuno-Matsumoto, Y., Yoshimine, T., Nii, Y., Kato, A., Taniguchi, M., Lee, J.K., Ko, T.S., Date, S., Tamura, S., Shimojo, S., Shinosaki, K., Inouye, T., Takeda, M., 2001. Landau–Kleffner syndrome: localization of epileptogenic lesion using wavelet cross-correlation analysis. Epilepsy and Behaviour 2, 288–294.

Mizuno-Matsumoto, Y., Motamedi, G.K., Webber, W.R.S., Lesser, R.P., 2002. Wavelet cross-correlation analysis can help predict whether bursts of pulse stimulation will terminate after discharges. Clinical Neurophysiology 113, 33–42.

Onorato, M., Salvetti, M.V., Buresti, G., Petagna, P., 1997. Application of a wavelet cross-correlation analysis to DNS velocity signals. European Journal of Mechanics B 16 (4), 575–597.

Pandey, G., Lovejoy, S., Schertzer, D., 1998. Multifractal analysis of daily river flows including extremes from basin of five to two million square kilometers, one day to 75 years. Journal of Hydrology 208, 62–81.

Papoulis, A., 1964. Probability, Random Variables and Stochastic Processes. McGrawHill, New York, NY, 588pp.

Pelletier, J.D., Turcotte, D.L., 1997. Long range persistence in climatological and hydrological time series: analysis, modelling and application to drought hazard assessment. Journal of Hydrology 203, 198–208.

Percival, D., 1995. On estimation of wavelet variance. Biometrika 82 (3), 619–631.

Percival, D., Mofjeld, H.O., 1997. Analysis of subtidal coastal sea level fluctuations using wavelets. Journal of the American Statistical Association 92 (493), 868–880.

Poggie, J., Smits, A.J., 1997. Wavelet analysis of wall-pressure fluctuations in a supersonic blunt-fin flow. AIAA Journal 35 (10), 1597–1603.

Priestley, M.B., 1981. Spectral analysis and time series. Academic Press, New York, 890pp.

Prokoph, A., Veizer, J., 1999. Trends, cycles and nonstationarities in isotope signals of phanerozoic seawater. Chemical Geology 161, 225–240.

Quiroga, R.Q., Rosso, O.A., Basar, E., Schurmann, M., 2001. Wavelet entropy in event-related potentials: a new method shows ordering of EEG oscillations. Biological Cybernetics 84, 291–299.

Rényi, A., 1976. Some fundamental questions of information theory. In Selected Papers of Alfred Rényi 2, 526–552.

Rosso, O.A., Mairal, M.L., 2002. Characterization of time dynamical evolution of electroencephalographic epileptic records. Physica A 312, 469–504.

Rosso, O.A., Martin, M.T., Plastino, A., 2003. Brain electrical activity analysis using a wavelet-based informational tool (II): Tsallis non-extensivity and complexity measures. Physica A 320, 497–511.

Shannon, C.E., 1946. A mathematical theory of communication. Bell System Technology Journal 27, 379–423, see also pp. 623–656.

Sello, S., 2003. Wavelet entropy and the multi peaked structure of solar cycle maximum. New Astronomy 1.

Sello, S., Bellazzini, J., 2000. Wavelet cross-correlation analysis of turbulent mixing from large-eddy simulations. Eighth European Turbulence Conference, Barcelona, Spain, 27–30, June 2000.

Singh, V.P., 2000. The entropy theory as a tool for modelling and decision making in environmental and water resources. Journal of the Water Society of America 1, 1–11.

Smith, L.C., Turcotte, D.L., Isacks, B.L., 1998. Stream flow characterization and feature detection using a discrete wavelet transform. Hydrological Processes 12, 233–249.

Sonuga, J.O., 1976. Entropy principle applied to the rainfall-runoff process. Journal of Hydrology 30, 81–94.

Strang, G., 1989. Wavelets and dilation equation: a brief introduction. SIAM Review 31 (4), 614–627.

Szilagyi, J., Parlange, M.B., Katul, G.G., Albertson, J.D., 1999. An objective method for determining principal time scales of coherent eddy structures using orthonormal wavelets. Advances in Water Resources 22 (6), 561–566.

Takeuchi, N., Narita, K., Goto, Y., 1994. Wavelet analysis of meteorological variables under winter thunderclouds over the Japan sea. Journal of Geophysical Research 99 (D5), 10751–70757.

Tessier, Y., Lovejoy, S., Hubert, P., Schertzer, D., Pecknold, S., 1996. Multifractal analysis and modeling of rainfall and river flows and scaling causal transfer functions. Journal of Geophysical Research 101 (D21), 26427–26440.

Torrence, C., Compo, G.P., 1998. A practical guide to wavelet analysis. Bulletin of the American Meteorological Society 79, 61–78.

Torrence, C., Webster, P.J., 1999. Interdecadal changes in the ENSO-monsoon system. Journal of Climate 12, 2679–2690.

Turner, B.J., Leclerc, M.Y., Gauthier, M., Moore, K.E., Fitzjarrald, D.R., 1994. Identification of turbulence structures above a forest canopy using a wavelet transform. Journal of Geophysical Research 99 (D1), 1919–1926.

Tyson, P.D., Cooper, G.R.J., McCarthy, T.S., 2002. Millenial to multi-decadal variability in the climate of Southern Africa. International Journal of Climatology 22, 1105–1117.

Venugopal, V., Foufoula-Georgiou, E., 1996. Energy decomposition of rainfall in the time–frequency–scale domain using wavelet packets. Journal of Hydrology 187, 3–27.

Walker, J.S., 1997. Fourier analysis and wavelet analysis. Notices of the American Mathematical Society 44 (6), 658–670.

Wessel, N., Schimann, A., Schirdewan, A., Voss, A., Kurths, J., 2000. Entropy measures in heart rate variability data. Lecture Notes in Computer Sciences 1933, 78–87.

Yokoyama, Y., Yamasaki, T., 2000. Geomagnetic paleointensity variation with a 100 kyr quasi-period. Earth and Planetary Science Letters 181, 7–14.

Yordanova, J., Kolev, V., Rosso, O.A., Schurmann, M., Sakowitz, O.W., Ozgoren, E., 2002. Wavelet entropy of event related potentials indicates modality-independent theta dominance. Journal of Neuroscience Methods 117, 99–109.